Properties of Liquid Silicon Observed by Time-Resolved X-Ray Absorption Spectroscopy

S. L. Johnson,[1,*] P. A. Heimann,[2] A. M. Lindenberg,[1] H. O. Jeschke,[3] M. E. Garcia,[3] Z. Chang,[4] R. W. Lee,[5]
J. J. Rehr,[6] and R. W. Falcone[1,7]

[1]*Department of Physics, University of California, Berkeley, California 94720, USA*
[2]*Advanced Light Source, Lawrence Berkeley National Laboratory, Berkeley, California 94720, USA*
[3]*Institut für Theoretische Physik, Freie Universität Berlin, Arnimallee 14, 14195 Berlin, Germany*
[4]*Department of Physics, Kansas State University, Manhattan, Kansas 66506, USA*
[5]*Lawrence Livermore National Laboratory, Livermore, California 94551, USA*
[6]*Department of Physics, University of Washington, Seattle, Washington 98195, USA*
[7]*Center for Beam Physics, Lawrence Berkeley National Laboratory, Berkeley, California 94720, USA*
(Received 13 November 2002; published 9 October 2003)

Time-resolved x-ray spectroscopy at the Si L edges is used to probe the electronic structure of an amorphous Si foil as it melts following absorption of an ultrafast laser pulse. Picosecond temporal resolution allows observation of the transient liquid phase before vaporization and before the liquid breaks up into droplets. The melting causes changes in the spectrum that match predictions of molecular dynamics and *ab initio* x-ray absorption codes.

The melting of solid, covalently bonded semiconductors into metallic liquids has attracted considerable attention due to both the technological importance of semiconductor processing and the peculiar nature of the liquids, which typically have much lower coordination numbers than do most liquid metals (6–7 vs 10–12) [1–3]. These lower coordination numbers presumably indicate a persistence of covalent bonding in the melt. Molecular dynamics simulations of molten Si suggest that approximately 30% of the bonds in liquid Si are covalent and that the bonding is a highly dynamic phenomenon, with bonds rapidly forming and breaking on a time scale of 20 fs [4]. Although x-ray and neutron diffraction experiments have accurately characterized the atomic structure of liquid Si [5,6], experimental investigation of the electronic structure is incomplete and may yield further insights.

X-ray spectroscopy is a powerful experimental means for investigating electronic structure. The high temperature and volatile nature of liquid Si are, however, not compatible with spectroscopic methods used for static samples. In our experiment, a short laser pulse (150 fs, 800 nm) rapidly heats and melts a thin amorphous Si foil, producing a sheet of liquid that persists while x rays probe absorption through the sample before the liquid vaporizes or breaks up into droplets. Previous time-resolved x-ray studies of laser-melted Si using nanosecond laser pulses have demonstrated large changes near the Si L edges [7,8], but relatively coarse temporal and spectral resolution prevented quantitative conclusions.

Our measurements employ picosecond resolution to study laser-heated amorphous Si foils. Figure 1 shows a sketch of relevant aspects of the setup at beam line 5.3.1 of the Advanced Light Source (ALS). A grazing incidence toroidal mirror focuses a broad spectrum of pulsed soft x-ray light from a synchrotron bend magnet to a 300 μm diameter spot on the foil. Before reaching the foil, the beam reflects from a pair of flat carbon-coated mirrors that serve as a low-pass photon energy filter, with the energy cutoff set by both the carbon K edge at 285 eV and the incidence angle θ of x rays on the mirrors. The x rays then strike the foil in the center of a 400 μm diameter laser-heated region. After passing through the foil, the x rays enter a spectrograph that uses a varied-line-spaced grating to create an energetically dispersed flat field image of the x-ray focus. The spectrograph diffracts the transmitted x rays into a spectrum ranging from 85 to 300 eV with a resolution of approximately 1 eV near the Si $L_{\mathrm{II,III}}$ edge at 100 eV. Proper adjustment of the angle θ of the carbon-coated mirrors suppresses higher-order grating reflections for a particular region of the spectrum, necessary because of the wide range of x-ray photon energies produced by the bend magnet.

Depending on the desired time resolution of the experiment, one of two types of detectors measures the resulting spectrum. For a resolution of 70 ps, we use a gated set of imaging microchannel plates coupled to a phosphor screen and charge-coupled device camera. The gate width of the plates is 20 ns, sufficient to isolate a single x-ray pulse from the ALS. By adjusting the relative timing of the laser and x-ray pulses, we obtain the spectrum as a function of time after excitation. The time resolution of this "pump-probe" technique is determined
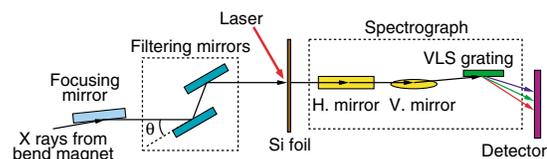
FIG. 1 (color online).   Sketch of setup at ALS beam line 5.3.1.

by the duration of the x-ray pulse. For better resolution, we employ an ultrafast x-ray streak camera to observe changes in intensity within the x-ray pulse [9]. This instrument can record changes in the transmission spectrum faster than 1 ps at the cost of some experimental complexity and decreased quantum efficiency.

Representative pump-probe data are shown in Fig. 2 for a 500 Å foil with an incident laser fluence of 0.7 J/cm^2. The dashed curve shows the absorption spectrum before excitation. This spectrum of the unheated foil agrees with previous measurements, allowing for a 30% error in the assumed areal density of the foils [10,11]. The large edge at 100 eV is a superposition of the L_{II} and L_{III} spin-orbit split edges, not separately distinguishable due to the spectrograph resolution. At 150 eV, the smaller L_I edge appears. Energies beyond 280 eV were inaccessible due to absorption from carbon.

The solid line in Fig. 2 shows the spectrum 100 ps after laser excitation. The laser affects the $L_{II,III}$ edge dramatically, reducing the size of the edge by 50% and increasing the width to 2 eV. In addition, the near-edge features of the $L_{II,III}$ edge are modified, the L_I edge shifts to lower energies by 1.6 ± 0.2 eV, and the small $L_{II,III}$ extended x-ray fine structure (EXAFS) oscillations beyond the L_I edge disappear [12]. These features do not change for longer pump-probe delays until about 10 ns after excitation. At this time, the overall transmission of the foil begins to increase, suggesting that material is starting to leave the probed region. This is consistent with experimental and theoretical work on femtosecond ablation indicating that the hydrodynamic evolution of the foil results in an expanding 1D liquid bubble with approximately constant temperature and density that persists for several nanoseconds [13,14].

As the incident laser fluence increases from zero, the changes in the near-threshold region of the $L_{II,III}$ edge take effect at approximately 0.1 J/cm^2, reaching a fluence-independent saturation level above 0.3 J/cm^2. This threshold value agrees with previous measurements on femtosecond melting in bulk Si [15], and the observed
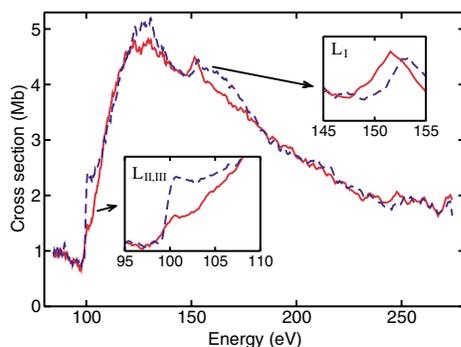
saturation at higher fluence suggests that under these conditions the probed region of the foil is completely melted. At the fluence of 0.7 J/cm^2 where all other reported measurements were performed, transreflectance measurements using an integrating sphere estimate a 40% absorption of the laser energy. Precise estimates of the temperature are difficult since even a fraction of the resulting 600 kJ/mol energy density causes the Si to approach its critical temperature near 5000 K, where the heat capacity increases rapidly as energy is used to break strong interatomic bonds [16].

To achieve higher time resolution of the changes in the $L_{II,III}$ edge, we employed the streak camera detector to measure the transmission spectrum of a 1000 Å foil with 5 ps resolution. To obtain better statistics, we integrated the signal over a 5 eV energy range above the edge. Figure 3 shows this integrated postedge absorption as a function of time after laser excitation. The absorption drop is instantaneous within the camera resolution. Further, the magnitude of the drop agrees with that observed in pump-probe measurements on 1000 Å foils (a smaller effect than in 500 Å foils, suggesting that the thicker foils are only partly melted even at 0.7 J/cm^2) [17]. These observations are consistent with ultrafast optical measurements, where a transition from the solid to a high reflectivity, electronically disordered phase occurs in 300 fs [15,18].

To obtain models for comparison with the x-ray data, we employed molecular dynamics (MD) simulations to calculate atomic structure and then used the *ab initio* x-ray absorption code FEFF 8.1 [19] to calculate absorption spectra from this structure. We performed the MD simulations on a block of 216 atoms initially in a crystalline configuration, with periodic boundary conditions in a fixed volume supercell. The system (atoms + electrons) was heated by a laser pulse, as described in [20,21], and then permitted to equilibrate for several picoseconds to 3100 K. The simulations used a tight-binding Hamiltonian with parameters from [22]. The pair correlation function of the resulting structure agrees with the

FIG. 2 (color online). Absorption spectra of the 500 Å foils before (dashed curve) and 100 ps after (solid curve) laser excitation. The plots are an average of about 100 laser/x-ray shots.
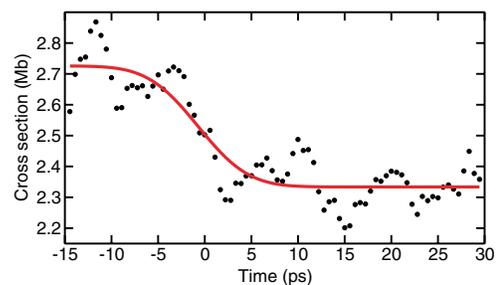
FIG. 3 (color online). Absorption of a 1000 Å Si foil immediately above the $L_{II,III}$ edge as a function of time after excitation. The circles show the average of 140 shots. The curve shows a fit to a step function convolved with a 5 ps FWHM Gaussian.

results of x-ray diffraction measurements on liquid Si near the melting temperature [5,6].

The FEFF calculations of the x-ray absorption spectra presented here use an initial state approximation. We also calculated the spectra using a fully statically screened core hole, but we found that this yields a poorer match to experiment for the near-edge structure of the solid Si $L_{II,III}$ edge in the range of 10–50 eV past the edge threshold, and it has little qualitative impact on the spectrum closer to the edges [23]. This static screening model neglects local field effects which tend to cancel the core-hole potential. This cancellation phenomenon is a particularly strong effect in the L edges of materials with low d occupation [24,25]. The dynamic screening model discussed in [25] should provide better results, but for the present work the initial state approximation (assuming complete cancellation of the core-hole potential and local field effects) appears adequate.

To extract spectra from the simulated structure, we ran FEFF on each of approximately 50 randomly selected atoms as x-ray absorbers. The code calculated the spectrum of each absorber using a cluster of radius 6.1 Å encompassing about 30 atoms. We then averaged together the individual spectra. We performed similar calculations on the spectrum of the initial solid using a published model structure of amorphous solid Si [26].

Figure 4 shows a comparison of the model results for the near-edge structure of the $L_{II,III}$ edge for both the initial solid and the liquid. For energies above 110 eV, the model calculations are close to experiment. The prominent feature in this energy range is a broad absorption maximum near 125 eV. The model shows a -4 eV shift in this feature on melting that is consistent with the experiment [27]. This energy shift and the associated reduction of the peak on melting are consequences of an expansion of the nearest-neighbor distance by 0.15 ±
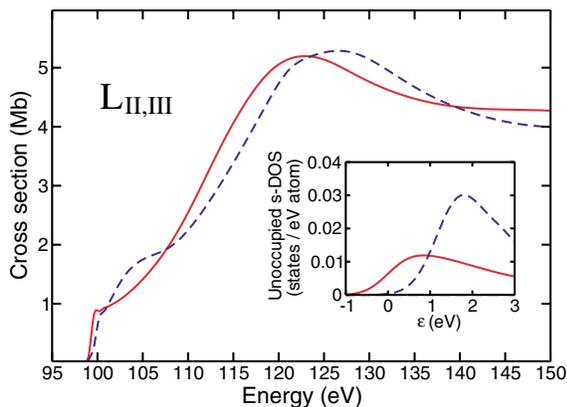
0.07 Å (compared against the 2.35 Å spacing in solid Si) and an increase in structural disorder. The onset of short-range disorder also suppresses EXAFS structure at higher energies via a reduction in the Debye-Waller factor $e^{-2\sigma^2 k^2}$, where σ is the variance of the bond length distribution and k is the photoelectron wave number, larger than 4 Å^{-1} for photon energies above 160 eV. Melting causes an increase in σ from 0.065 Å at room temperature [28] to 0.25 Å, reducing the EXAFS amplitude to below the noise level.

Closer to the edge threshold, the agreement is mostly qualitative, possibly due to neglect of nonspherical components of the electron potential in FEFF [29]. The MD calculations show that the melting of Si causes a "flattening" of the density of states (DOS) near the Fermi level and an associated collapse of the semiconductor band gap. This change in the DOS manifests itself in the spectra as a reduction in the near-threshold absorption, evident in both the model spectra and the experimental data. The inset of Fig. 4 shows plots of the 3s-projected unoccupied DOS. Although the curve for the solid shows significant structure (a dip at the Fermi level followed by a peak at higher energies), the unoccupied 3s-DOS of the liquid is essentially featureless beyond the consequences of simple state filling. These curves compare favorably to the observed near-threshold absorption. This agreement persists even though such a comparison ignores both contributions to the edge structure from other unoccupied states permitted by selection rules and the potentially important core-hole effects that have been shown in crystalline Si to shift the $L_{II,III}$ edge by -1 eV [30]. The 2 eV edge broadening observed for the liquid $L_{II,III}$ edge but not reproduced by the modeling may result from simultaneously probing a wide range of liquid densities in the experiment. By running FEFF on uniform dilations and contractions of the liquid model structure, we estimated that a 30% distribution of densities around the density of the liquid model is sufficient to cause a 2 eV edge broadening because of shifts in the Fermi level with respect to the 2p core levels. This wide density distribution also broadens and reduces by 5% the absorption maximum near 125 eV, bringing it closer to the experimental observations. Such a large variation in density might be explained by nonuniformities of energy deposition along the 300 μm x-ray spot size, or perhaps by the large local density fluctuations expected in liquids when pushed to temperatures near the critical point [16,31]. Extending the MD simulations to higher temperatures could provide further insight.

Calculations on the L_I edge are shown in Fig. 5. Although the models for both solid and liquid Si show edge thresholds that differ from experimental values by about 5 eV, the model spectra do show an edge shift of approximately -1.2 eV from the solid to the liquid due to band gap collapse, close to the observed -1.6 ± 0.2 eV shift. The unoccupied 3p-DOS plotted in the inset of Fig. 5 shows a similar shift of -1.1 eV. Like the changes

FIG. 4 (color online). Comparison of FEFF calculations for liquid Si (solid curve) and unheated Si (dashed curve) near the $L_{II,III}$ edge. The inset shows the unoccupied 3s-DOS from the MD simulations, convolved with a 1 eV FWHM Gaussian to approximate experimental resolution. The zero of the electron energy ϵ is set to the calculated Fermi level of the liquid.
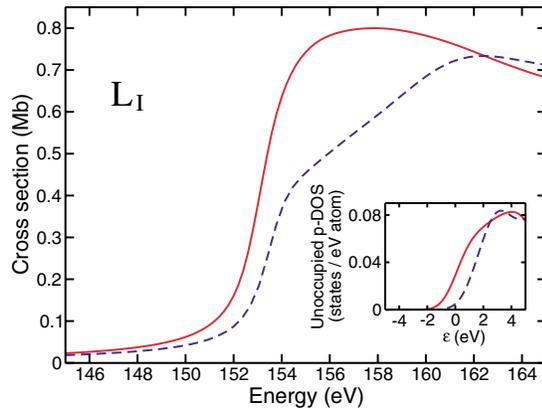
FIG. 5 (color online). Comparison of FEFF calculations for the liquid (solid curve) and unheated Si (dashed curve) near the L_I edge. The inset shows the unoccupied $3p$-DOS from the MD simulations, convolved with a 2 eV FWHM Gaussian.

in the near-edge structure of the $L_{II,III}$ edge, the L_I edge shift appears to be at least partly due to collapse of the semiconductor band gap on melting. Note that, compared to the $L_{II,III}$ edge, the L_I edge is less sensitive to broadening effects from density variations because of its already large lifetime and instrumental broadening.

By comparing the entirety of the model calculations with the data, we conclude that the high-temperature liquid Si produced by the laser is a structurally disordered metal with a nearest-neighbor distance in agreement with that previously measured for liquid Si near the melting temperature. Although agreement between experiment and the model is already quite good, further improvement might result from a more sophisticated treatment of final-state effects and by extending the MD simulations to even higher temperatures to explore the effects of near-critical local density fluctuations. This work has demonstrated a new technique for studying volatile, high-temperature, near solid-density materials using x-ray absorption spectroscopy. The combination of short-pulse laser sources and temporally resolved x-ray absorption spectroscopy offers potential to explore the electronic structure of materials under temperatures and pressures inaccessible by other means.

*Electronic address: Steve.Johnson@mailaps.org

[1] P. S. Salmon, J. Phys. F **18**, 2345 (1988).
[2] V. Petkov, S. Takeda, Y. Waseda, and K. Sugiyama, J. Non-Cryst. Solids **168**, 97 (1994).
[3] B. C. Larson et al., Appl. Phys. Lett. **42**, 282 (1983).
[4] I. Štich, R. Car, and M. Parrinello, Phys. Rev. Lett. **63**, 2240 (1989).
[5] Y. Waseda and K. Suzuki, Z. Phys. B **20**, 339 (1975).
[6] J. P. Gabathuler and S. Steeb, Z. Naturforsch. Teil A **34**, 1314 (1979).
[7] K. Murakami et al., Phys. Rev. Lett. **56**, 655 (1986).
[8] H. C. Gerritsen et al., J. Appl. Phys. **60**, 1774 (1986).
[9] Z. Chang et al., Appl. Phys. Lett. **69**, 133 (1996).
[10] F. C. Brown and O. P. Rustigi, Phys. Rev. Lett. **28**, 497 (1972).
[11] F. C. Brown, R. Z. Bachrach, and M. Skibowski, Phys. Rev. B **15**, 4781 (1977).
[12] The disappearance of EXAFS oscillations past the L_I edge is confirmed by a phase-corrected fast Fourier transform of the data, showing that melting pushes the nearest-neighbor peak below the noise level.
[13] K. Sokolowski-Tinten, J. Bialkowski, A. Cavalleri, and D. von der Linde, Phys. Rev. Lett. **81**, 224 (1998).
[14] S. I. Anisimov et al., Appl. Phys. A **69**, 617 (1999).
[15] M. C. Downer and C. V. Shank, Phys. Rev. Lett. **56**, 761 (1986).
[16] A. Miotello and R. Kelly, Appl. Phys. A **69**, S67 (1999).
[17] Note also that, due to uncertainties in the assumed areal density of the foils, the plotted absolute cross section of the 1000 Å foil is 10% higher than that of the 500 Å foils.
[18] H. W. K. Tom, G. D. Aumiller, and C. H. Brito-Cruz, Phys. Rev. Lett. **60**, 1438 (1988).
[19] A. L. Ankudinov, B. Ravel, J. J. Rehr, and S. D. Conradson, Phys. Rev. B **58**, 7565 (1998).
[20] H. O. Jeschke et al., Appl. Surf. Sci. **197–198**, 839 (2002).
[21] H. O. Jeschke, M. E. Garcia, and K. H. Bennemann, Phys. Rev. Lett. **87**, 015003 (2001).
[22] I. Kwon et al., Phys. Rev. B **49**, 7242 (1994).
[23] In particular, we did not observe any significant edge shift of either the $L_{II,III}$ or L_I edges when turning on final-state relaxation.
[24] A. I. Nesvizhskii and J. J. Rehr, J. Synchrotron Radiat. **6**, 315 (1999).
[25] A. L. Ankudinov, A. I. Nesvizhskii, and J. J. Rehr, Phys. Rev. B **67**, 115120 (2003).
[26] G. T. Barkema and N. Mousseau, Phys. Rev. B **62**, 4985 (2000).
[27] An experimental shift of -4 ± 2 eV was estimated by using the model curves as a guide to the shape of the absorption, performing small contractions and dilations of the underlying structure as a fitting parameter. This is also how we estimate uncertainty in the change of the nearest-neighbor distance.
[28] K. Laaziri et al., Phys. Rev. B **60**, 13 520 (1999).
[29] J. J. Rehr and R. C. Albers, Rev. Mod. Phys. **72**, 621 (2000).
[30] R. Buczko, G. Duscher, S. J. Pennycook, and S. T. Pantelides, Phys. Rev. Lett. **85**, 2168 (2000).
[31] M. M. Martynyuk, Sov. Phys. Tech. Phys. **19**, 793 (1974).